Journal of Molecular Catalysis A: Chemical 348 (2011) 70–76

Contents lists available at SciVerse ScienceDirect

Journal of Molecular Catalysis A: Chemical

journal homepage: www.elsevier.com/locate/molcata

Efficient degradation of pyruvic acid in water by catalytic ozonation with PdO/CeO_2

Weiwei Li, Zhimin Qiang*, Tao Zhang, Xiaolei Bao, Xu Zhao

State Key Laboratory of Environmental Aquatic Chemistry, Research Center for Eco-Environmental Sciences, Chinese Academy of Sciences, 18 Shuang-qing Road, Beijing 100085, China

ARTICLE INFO

Article history:
Received 21 April 2011
Received in revised form 11 August 2011
Accepted 13 August 2011
Available online 22 August 2011

Keywords:
PdO/CeO_2
Surface property
Catalytic activity
Pyruvic acid
Ozonation

ABSTRACT

PdO/CeO_2 prepared at various calcination temperatures and Pd loading percentages significantly enhanced the degradation of pyruvic acid (PA) in water by catalytic ozonation compared to ozonation alone. The surface property of PdO/CeO_2 was characterized with X-ray diffraction, transmission electron microscope, X-ray photoelectron spectroscopy, BET surface area and zeta potential, and its relationship with the catalytic activity was examined and discussed in detail. Results indicate that PdO/CeO_2 with 4.0% of Pd loading and calcined at 550 °C showed the highest catalytic activity in PA degradation by ozone. Complete PA ($5\,mg\,L^{-1}$) removal was quickly achieved in catalytic ozonation at 5 min and pH 4.7, in which PdO and CeO_2 exerted a synergic effect. Moreover, PdO/CeO_2 exhibited a persistently high activity throughout the semi-continuous ozonation of PA. It was observed that the surface contents of Ce(III) and Pd(II) were closely related to the catalytic activity and the optimal surface molar ratio of Ce(III)/Pd(II) was around 1:1. The positively charged surface of PdO/CeO_2 also played an important role in catalyzing PA degradation by ozone.

1. Introduction

Ozonation has been widely used for organic pollutants removal from water and wastewater. Ozone is reactive towards many organic pollutants, especially those containing aromatic rings, double bonds, and amine- or sulfur-moieties [1,2]. However, the reaction rates between ozone and a significant amount of other organic pollutants are rather low, making them difficult to degrade during ozonation. Among these organics, ozonation by-products such as small carboxylic acids, ketones and aldehydes are hardly reactive to ozone [3,4]. Pyruvic acid (PA), a major by-product formed during the ozonation of water containing dissolved aromatic compounds or natural organic matter, is quite resistant to further oxidation by ozone ($k = 0.025\,min^{-1}$) [5]. Thus, heterogeneous catalytic ozonation has been studied to promote the oxidation of PA in recent years. It was reported that Co/Al_2O_3 [6], MnO_2 and Mn^{2+} ions [7], $CuO/ZrO_2–Al_2O_3$ [8], perovskite ($LaTi_{0.15}Cu_{0.85}O_3$) [9] and activated carbon [5] could catalyze PA degradation by ozone. However, most of these works focused on the influence of experimental conditions (e.g., pH, ozone dose, contact time) on PA removal while the relationship between the surface property and catalytic activity of the studied catalysts was much less concerned. Alvarez et al. [6] investigated the structural characteristics of Co/Al_2O_3 used for the catalytic ozonation of PA and found that the different surface Co phases showed different catalytic activities. The catalyst with Co_3O_4 as the main Co phase was the most active, achieving about 28% removal of PA at 20 min and pH 2.5 in catalytic ozonation.

In this study, we found that PdO/CeO_2 prepared at various calcination temperatures and Pd loadings was efficient in promoting the degradation of PA by ozone at elevated pH values (i.e., pH 4.7–6.0), which may favor its application in water treatment. In addition, through detailed examination of the property–activity relationship, the important surface properties governing the catalytic activity of PdO/CeO_2 were proposed.

2. Experimental

2.1. Catalyst preparation

CeO_2 was synthesized by urea-hydrothermal means with certain modification [10]. Specifically, $Ce(NO_3)_3{\cdot}6H_2O$ and urea were co-dissolved in distilled water with a molar ratio of 1:3. The mixture was then transferred to a sealed stainless steel vessel and heated at 140 °C for 5 h. After filtration and repeated washings, the precipitate was dried at 120 °C for 2 h and calcined at 450 °C for 4 h. The diameter of CeO_2 particles was mainly in the range of 0.6–7.7 μm.

---

* Corresponding author. Tel.: +86 10 62849632; fax: +86 10 62849659.
E-mail address: qiangz@rcees.ac.cn (Z. Qiang).

1381-1169/$ – see front matter © 2011 Elsevier B.V. All rights reserved.
doi:10.1016/j.molcata.2011.08.003

PdO/CeO_2 was prepared by impregnating CeO_2 with $Pd(NO_3)_2$ aqueous solution according to the incipient wetness method with some modification [11]. The calculated Pd content (wt.%) loaded on the catalyst ranged from 0.6% to 4.7%. The impregnated samples were dried at 60 °C and finally calcined in air for 3 h at temperatures ranging from 400 to 800 °C. The heating rate was 2 °C min^{-1} in all calcinations. The prepared catalysts were designated as PdO/CeO_2-*X*%-*Y*°C, where *X* refers to the weight percentage of Pd and *Y* to the calcination temperature.

2.2. Catalyst characterization

The morphology of catalysts was visualized using transmission electron microscope (TEM) (H-7500, Hitachi, Japan). The BET surface area was determined by adsorption and desorption of N_2 on a Micromeritics ASAP2000 analyzer. X-ray powder diffraction (XRD) measurement was carried out using a Bruker D8 Advance X-diffractometer (Cu Kα, $\lambda = 0.15406$ nm). The surface molar percentages of Pd and Ce were determined by X-ray photoelectron spectroscopy (XPS) with an Escalab 250 spectrometer (Thermofisher), and the XPS data corresponding to Ce 3d and Pd 3d spectra were fitted with Peakfit software (V4.12). The molar percentages of Ce and Pd of different valences with respect to the total Ce and Pd, respectively, were also analyzed from the XPS data. Zeta potential was determined by a Malvern zetameter (2000, Zetasizer). The particle size was measured with a laser particle size analyzer (2000, Mastersizer) in water.

2.3. Experimental procedures

Experiments were conducted in a 1-L cylindrical glass reactor with temperature controlled at 22 °C under magnetic agitation. The reactor was installed with an inlet and an outlet for ozone gas and sampling accessories. In a typical experiment, 500 mL aqueous suspension of PA (buffered with 10 mM borate) and 0.15 g catalyst were added into the reactor. Ozone, generated from dried oxygen with an ozone generator (3S-A5, Tonglin Technology, Beijing), was continuously bubbled into the reactor at a flow rate of 4 L min^{-1} and a gaseous concentration of 1.4 mg L^{-1}. Aqueous ozone concentration was determined with the indigo method [12]. Samples withdrawn at specific time intervals were filtered with 0.45-μm synthetic fiber filters after the residual ozone had been immediately quenched by Na_2SO_3. PA was analyzed on a high-performance liquid chromatograph (HPLC) (1200, Agilent) equipped with an Atlantis dC18 column and a UV detector at 215 nm. The mobile phase (0.8 mL min^{-1}) was a mixture of 10 mM NaH_2PO_4 solution (adjusted to pH 2.8) and methanol (V:V = 95:5).

3. Results

3.1. Catalyst characterization

3.1.1. Catalyst structure

The XRD patterns of CeO_2 and PdO/CeO_2 catalysts prepared in this work are shown in Fig. 1. PdO/CeO_2 with different Pd loadings calcined at temperatures no higher than 550 °C showed a characteristic cubic fluorite structure of CeO_2. When the calcination temperature was raised up to 650 °C and especially 800 °C, a peak at $2\theta = 33.9°$ emerged that is typical for the (1 0 1) diffraction of PdO [13]. The result indicates that PdO was well dispersed on the CeO_2 surface at lower calcination temperatures, while agglomerated at higher temperatures. With the Scherrer formula [14], the crystallite sizes of the catalysts were calculated to be within the range of 9.0–12.8 nm.

The TEM picture (Fig. 2A) shows that CeO_2 mainly existed in the form of nanorods. The catalysts with Pd loadings from 1.8% to 4.7% maintained the nanorods form (Figs. 2B–D). The PdO/CeO_2 particles appeared somewhat larger than CeO_2, possibly due to the uniform deposition of PdO. Unlike the PdO/CeO_2 calcined at relatively lower temperatures such as 550 °C (Fig. 2E), the one calcined at 800 °C showed an obvious crystallite agglomeration, forming irregular-shaped particles (Fig. 2F).

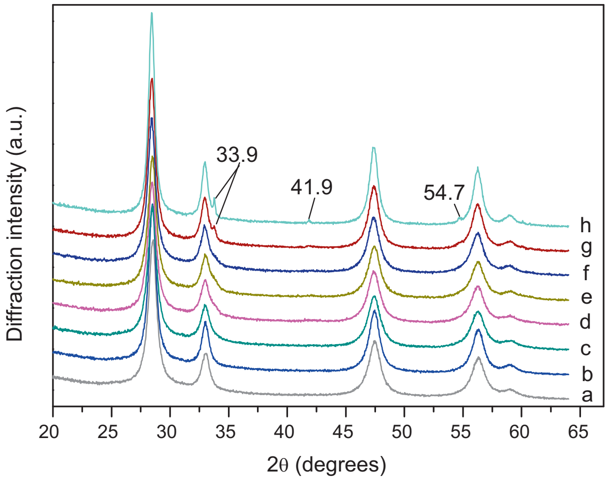

Fig. 1. XRD patterns of CeO_2 and PdO/CeO_2: (a) CeO_2; (b) PdO/CeO_2-0.6%-400 °C; (c) PdO/CeO_2-1.8%-400 °C; (d) PdO/CeO_2-4.0%-400 °C; (e) PdO/CeO_2-4.7%-400 °C; (f) PdO/CeO_2-4.0%-550 °C; (g) PdO/CeO_2-4.0%-650 °C; and (h) PdO/CeO_2-4.0%-800 °C.

3.1.2. Surface elemental composition and BET surface area

Table 1 shows the surface molar percentages of Ce and Pd and the BET surface areas of PdO/CeO_2 prepared at various calcination temperatures and Pd loadings. The surface molar percentage of Ce gradually increased as the calcination temperature increased from 400 to 800 °C, whereas that of Pd generally decreased, which was probably ascribed to the release of lattice oxygen from CeO_2 and the clustering of PdO particles. Calcination at temperatures higher than 550 °C led to a significant decrease in the BET surface area, which could also be attributed to the particle clustering as shown in the TEM picture (Fig. 2F). However, the BET surface area was almost independent of the Pd loading in the studied range of 0.6–4.7%.

3.2. Catalytic ozonation of PA with PdO/CeO_2

3.2.1. Influence of calcination temperature

Only 26% of PA was degraded in ozonation alone at pH 4.7 at 20 min (Fig. 3A). The presence of PdO/CeO_2 significantly promoted PA degradation and the catalysts calcined at lower temperatures (e.g., 400 and 550 °C) were more active. The highest PA degradation rate (e.g., 100% removal at 5 min) was observed for PdO/CeO_2 calcined at 550 °C, which was slightly higher than that for PdO/CeO_2 calcined at 400 °C (e.g., 99% at 5 min). As the calcination temperature was further raised, the catalytic activity of PdO/CeO_2

Table 1
Surface elemental compositions and BET surface areas of CeO_2 and PdO/CeO_2.

Catalysts	Ce (at.%)	Pd (at.%)	Ce/Pd	BET surface area ($m^2\,g^{-1}$)
CeO_2	10.5			108
PdO/CeO_2-4.0%-400 °C	7.5	4.7	1.6	90
PdO/CeO_2-4.0%-550 °C	8.0	5.4	1.5	94
PdO/CeO_2-4.0%-650 °C	9.7	3.7	2.6	80
PdO/CeO_2-4.0%-800 °C	10.4	3.0	3.4	51
PdO/CeO_2-0.6%-400 °C	10.6	1.2	8.6	90
PdO/CeO_2-1.8%-400 °C	9.2	2.6	3.5	95
PdO/CeO_2-4.7%-400 °C	6.7	9.3	0.7	92

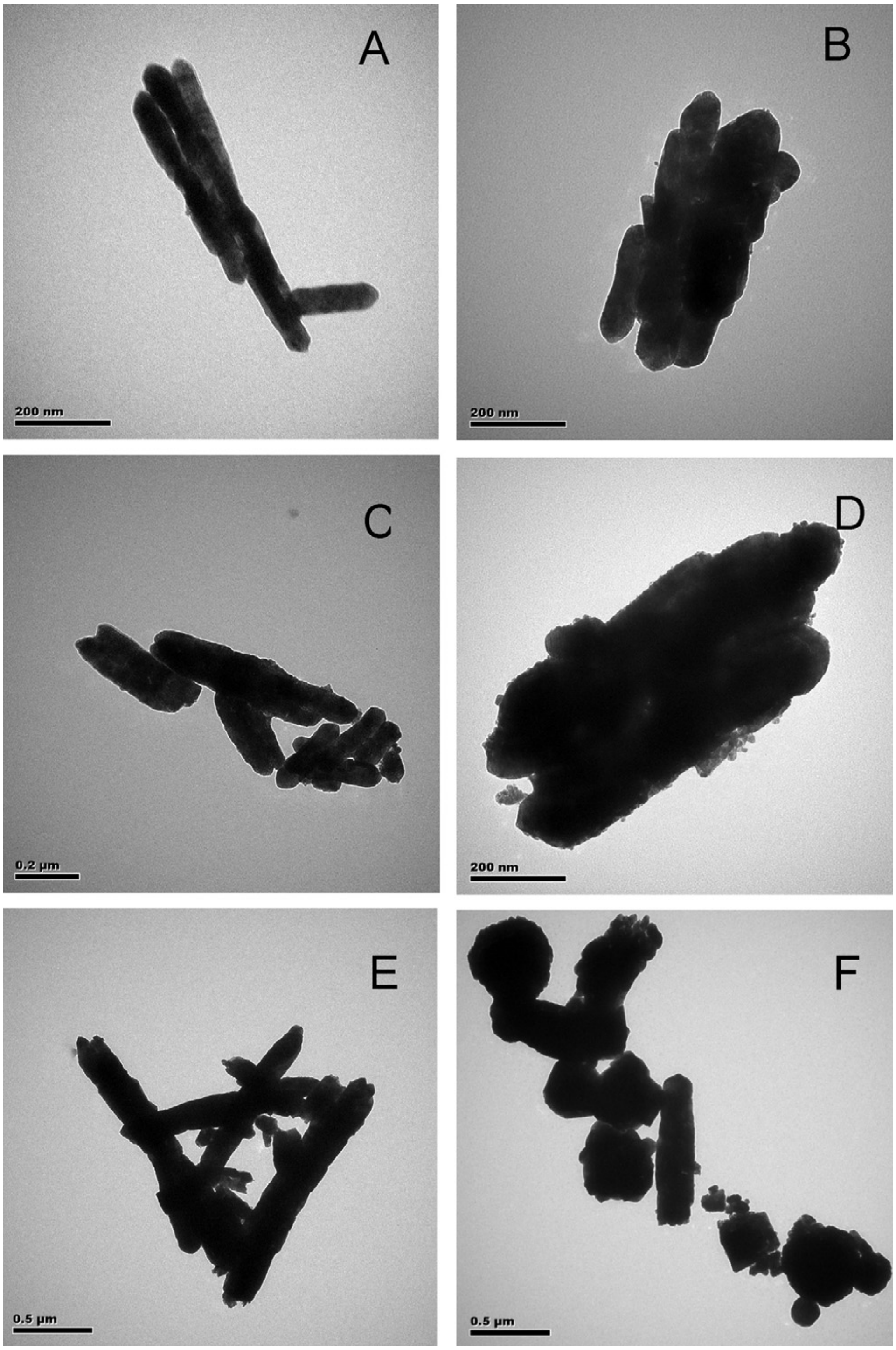

Fig. 2. TEM pictures: (A) CeO_2; (B) PdO/CeO_2-1.8%-400 °C; (C) PdO/CeO_2-4.0%-400 °C; (D) PdO/CeO_2-4.7%-400 °C; (E) PdO/CeO_2-4.0%-550 °C; (F) PdO/CeO_2-4.0%-800 °C.

decreased. However, PA was still removed by 81% in the presence of PdO/CeO_2-4.0%-800 °C at 20 min of reaction. The PA removal by PdO/CeO_2 adsorption alone was much lower (Fig. 3B), indicating that PA was mainly degraded via catalytic ozonation. It is noted that the catalytic activity of PdO/CeO_2 calcined at different temperatures was not positively related to its adsorption capacity for PA. For example, PdO/CeO_2-4.0%-400 °C and PdO/CeO_2-4.0%-550 °C removed 42% and 20% of PA in adsorption alone at 20 min, respectively, but the latter catalyst exhibited a higher PA degradation rate in catalytic ozonation.

3.2.2. *Influence of Pd loading*

The catalytic activity of CeO_2 was quite low since only 31% of PA was removed at 5 min in O_3/CeO_2 oxidation (Fig. 4A). The increase of Pd loading on CeO_2 from 0.6% to 4.0% led to a substantial increase in the PA degradation efficiency (e.g., from 60% to 99% at 5 min), indicating that Pd was an active species in PdO/CeO_2 for catalytic ozonation. Further increase of Pd loading to 4.7% led to a notable decrease in the degradation rate of PA. Therefore, the optimal Pd loading for the catalytic ozonation of PA was about 4.0%. Similar to CeO_2, PdO, which was added at the same dosage as

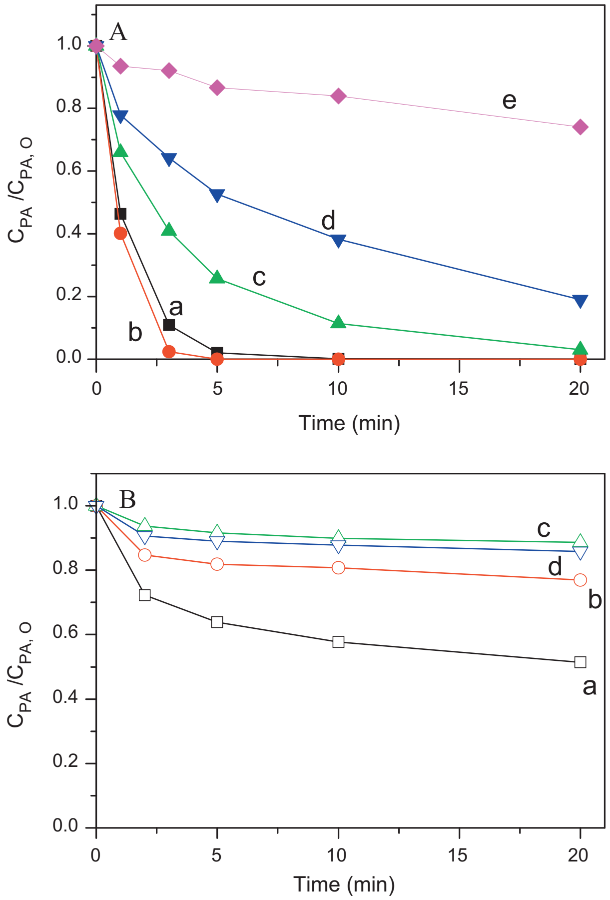

Fig. 3. PA degradation by ozonation alone and catalytic ozonation (A) and adsorption (B) with PdO/CeO_2 calcined at different temperatures: (a) PdO/CeO_2-4.0%-400 °C; (b) PdO/CeO_2-4.0%-550 °C; (c) PdO/CeO_2-4.0%-650 °C; (d) PdO/CeO_2-4.0%-800 °C; and (e) ozonation alone. Experimental conditions: aqueous ozone concentration = 1.0 mg L^{-1}, $[PA]_o = 5.0 \pm 0.5$ mg L^{-1}, catalyst dose = 300 mg L^{-1}, pH = 4.7, and $T = 22$ °C.

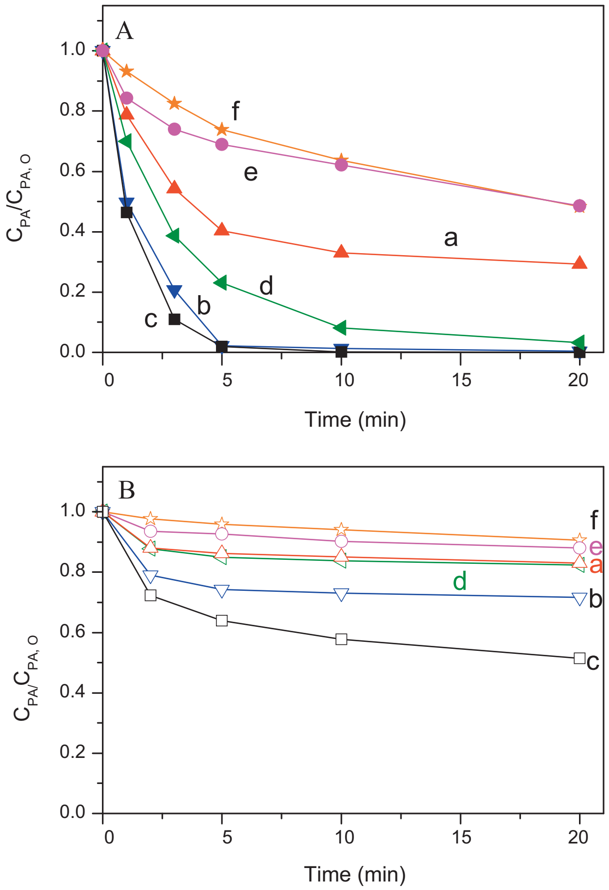

Fig. 4. PA degradation by catalytic ozonation (A) and adsorption (B) with CeO_2, PdO, and PdO/CeO_2 with different Pd loadings: (a) PdO/CeO_2-0.6%-400 °C; (b) PdO/CeO_2-1.8%-400 °C; (c) PdO/CeO_2-4.0%-400 °C; (d) PdO/CeO_2-4.7%-400 °C; (e) CeO_2; and (f) PdO. Experimental conditions: aqueous ozone concentration = 1.0 mg L^{-1}, $[PA]_o = 5.0 \pm 0.5$ mg L^{-1}, catalyst dose = 300 mg L^{-1} (except PdO = 16.2 mg L^{-1}), pH = 4.7, and $T = 22$ °C.

PdO/CeO_2-4.7%-400 °C in terms of the Pd content (wt.%), also showed a low activity in catalytic ozonation. Thus, the two constituent metal oxides should have a synergetic effect on the catalytic ozonation of PA. It is noted that the catalytic activity of PdO/CeO_2 (Fig. 4A), in terms of Pd loading, was consistent with its adsorption capacity for PA (Fig. 4B), i.e., the one that achieved a higher PA degradation rate in catalytic ozonation also showed a relatively higher PA removal in adsorption alone. Therefore, the adsorption of PA onto the metal oxides (calcined at the same temperature), which was probably pertinent to the Pd loading, seemed important for the catalytic ozonation. In addition, PdO/CeO_2 exhibited a higher adsorption capacity for PA than either CeO_2 or PdO (Fig. 4B), implying that the synergetic function existed between PdO and CeO_2 in the adsorption process.

3.2.3. *Influence of pH*

Since PA dissociation and adsorption onto metal oxides, ozone decomposition, and the surface charging state of metal oxides are all closely dependent on solution pH, there is no doubt that pH would significantly affect PA degradation in catalytic ozonation. Fig. 5 shows the PA degradation in ozonation and catalytic ozonation at different pHs. Results indicate that the degradation of PA by ozonation alone was higher at acidic and alkaline pHs (i.e., 3.0, 4.7, 8.8) than that at around neutral pHs (i.e., 6.0, 7.4) (Fig. 5A). PA removal at 20 min increased from 4% to 25% as pH was raised from 6.0 to 8.8, and from 4% to 67% as pH was decreased from 6.0 to 3.0. It is known that OH^- can initiate ozone decomposition to generate hydroxyl radicals ($^{\bullet}OH$), so the yield of $^{\bullet}OH$ will be substantially enhanced during ozonation at an alkaline pH. However, the degradation rate of PA was still low at pH 8.8, indicating that the indirect oxidation via $^{\bullet}OH$ was not effective for PA degradation. In contrast, the degradation of PA was remarkably enhanced at pH 3.0 due to the availability of abundant hydrogen ions (H^+). H^+ was consumed in the direct ozonation of PA, as evidenced by the fact that the solution pH was elevated from 3.0 to 3.6 when the reaction was complete.

It is also noticed that the PA degradation in catalytic ozonation increased substantially as the initial pH changed from 8.8 to 3.0 (Fig. 5B). In fact, PdO/CeO_2 did not show any catalytic activity at pH 8.8, as the removal of PA in catalytic ozonation was similar to that in ozonation alone. However, the removal of PA was enhanced from 7% in ozonation alone (Fig. 5A) to 45% in catalytic ozonation (Fig. 5B) at pH 7.4 as well as from 4% to 89% at pH 6.0, which may favor its application in water treatment. Nearly complete removal of PA was achieved within 5 and 1 min at pHs 4.7 and 3.0, respectively. Similar to ozonation alone, H^+ greatly promoted the degradation of PA in the catalytic ozonation. Rivas et al. [9] proposed the following reaction to explain the enhanced degradation of PA by ozone in the presence of perovskite ($LaTi_{0.15}Cu_{0.85}O_3$) under acidic conditions:

$$CH_3COCOOH + 2O_3 + 2H^+ \rightarrow CH_3COOH + CO_2 + 2O_2 + H_2O \quad (1)$$

Therefore, it is clear that the catalytic activity of PdO/CeO_2 was closely pH-dependent.

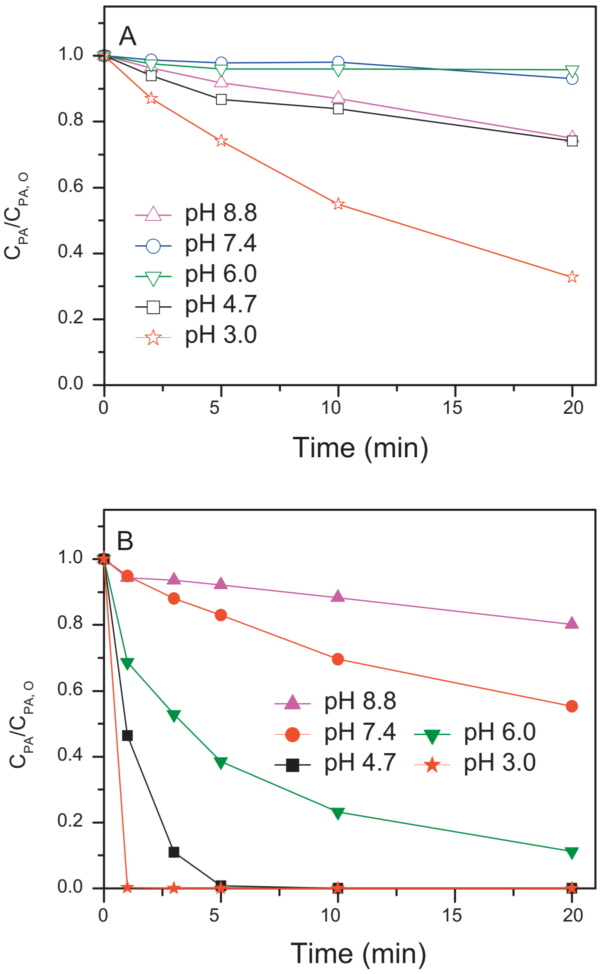

Fig. 5. Ozonation (A) and catalytic ozonation (B) of PA with PdO/CeO_2-4.0%-400 °C at different pHs. Experimental conditions: aqueous ozone concentration = 1.0 mg L^{-1}, $[PA]_o = 5.0 \pm 0.5$ mg L^{-1}, catalyst dose = 300 mg L^{-1}, and $T = 22$ °C.

3.2.4. *Byproduct identification*

Acetic acid was the only byproduct identified in both ozonation alone and catalytic ozonation. Fig. 6 shows that the molar yield of acetic acid, as quantified by HPLC, closely matched the consumption of PA. The concentrations of TOC were measured and then compared with those calculated from the contributions of PA and acetic acid (i.e., TOC_{cal}) at different reaction times. Results indicate that the measurement agreed well with the calculation. It is seen that along with the conversion of PA to acetic acid and CO_2, TOC was removed accordingly.

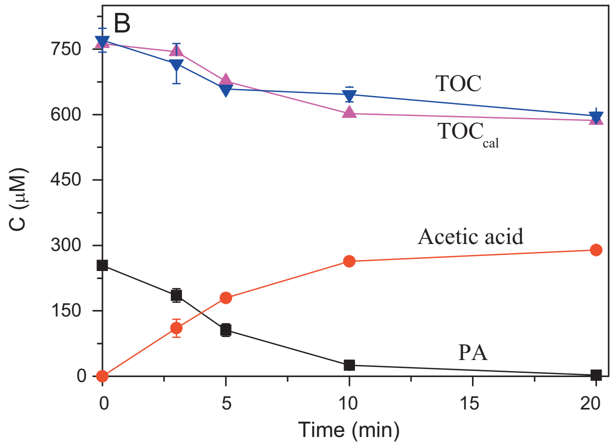

Fig. 6. Change of TOC, PA and acetic acid concentrations during catalytic ozonation of PA with PdO/CeO_2-4.0%-400 °C. Experimental conditions: aqueous ozone concentration = 1.0 mg L^{-1}, catalyst dose = 300 mg L^{-1}, pH = 4.7, and $T = 22$ °C.

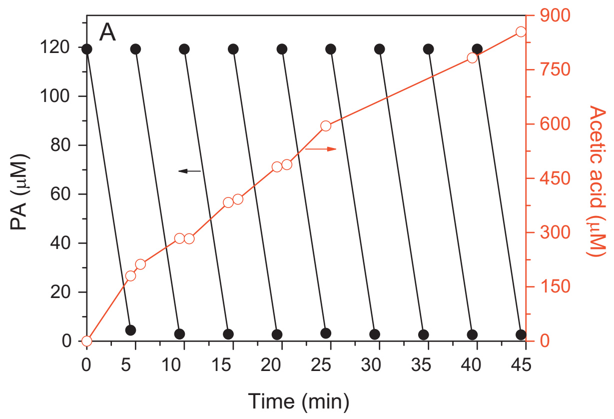

Fig. 7. Semi-continuous catalytic ozonation of PA with PdO/CeO_2-4.0%-400 °C. Experimental conditions: aqueous ozone concentration = 1.0 mg L^{-1}, catalyst dose = 500 mg L^{-1}, pH = 4.7, and $T = 22$ °C. PA (10.5 mg L^{-1}) was intermittently added every five minutes.

3.2.5. *Semi-continuous catalytic ozonation of PA with PdO/CeO_2*

Semi-continuous mode was adopted to examine the persistence of PdO/CeO_2-4.0%-400 °C. The reaction solution was continuously bubbled with ozone gas and the catalyst dosage was 500 mg L^{-1}. The same amount of PA (about 119.3 μM, or 10.5 mg L^{-1}, with respect to the reaction solution) was intermittently added into the reactor every five minutes. Results indicate that the removal of PA had little decline during the whole reaction course, indicating a persistently high activity of the catalyst (Fig. 7). After the reaction, the leached Pd and Ce concentrations in the aqueous solution were determined to be 0.89 and 23.12 μg L^{-1}, respectively, which approximately accounted for 0.005% and 0.006% of the total Pd and Ce in the catalyst. Therefore, PdO/CeO_2 also exhibited a high structural stability during the catalytic ozonation.

4. Discussion

4.1. *Surface elemental composition and catalytic activity*

It is known that CeO_2 is an excellent oxygen buffer due to its redox capacity arising from the flip–flop interaction between Ce(IV) and Ce(III) [15]. Because of the oxygen vacancies, a certain amount of Ce(III) usually exists in CeO_2. Likewise, the multi-valences of Pd, i.e., Pd(II) and Pd(IV), also co-exist in PdO. The molar percentages of the two surface metals at each valence can be estimated by analyzing the XPS data. According to Faria et al. [16], the Ce 3d spectrum can be deconvoluted to 10 peaks (6 for Ce(IV) and 4 for Ce(III)) in total, and the molar ratio of Ce(III) to the total Ce on the catalyst surface is equal to the ratio of their corresponding peak areas. Thus, the molar percentages of the surface Ce and Pd at different valences with respect to the total elements on PdO/CeO_2 surface can be calculated from their specific molar ratios and their surface elemental composition data (Table 1), which are summarized in Table 2.

For PdO/CeO_2 calcined at different temperatures, the molar percentage of Ce(IV) increased while that of Pd(II) decreased as the calcination temperature was raised from 400 to 800 °C (Table 2). In contrast, the molar percentages of both Ce(III) and Pd(IV) reached maximum at 550 °C. For the PdO/CeO_2 prepared with different Pd loadings, the molar percentage of Ce(IV) decreased from 9.0% to 5.3% as the Pd loading increased from 0.6% to 4.7%, while that of

Table 2
Molar percentages (at.%) of Ce and Pd of different valences with respect to the total elements on PdO/CeO_2 surface.

Catalysts	Ce(IV)	Ce(III)	Pd(IV)	Pd(II)	Ce(III)/Pd(II)
CeO_2	6.9	3.6			
PdO/CeO_2-4.0%-400 °C	5.4	2.1	1.6	3.1	0.7
PdO/CeO_2-4.0%-550 °C	5.4	2.5	3.0	2.4	1.0
PdO/CeO_2-4.0%-650 °C	7.6	2.0	2.1	1.6	1.3
PdO/CeO_2-4.0%-800 °C	8.6	1.8	2.8	0.9	2.0
PdO/CeO_2-0.6%-400 °C	9.0	1.7	0.7	0.5	3.4
PdO/CeO_2-1.8%-400 °C	7.5	1.7	0.9	1.7	1.0
PdO/CeO_2-4.7%-400 °C	5.3	1.4	5.4	3.8	0.4

Ce(III) reached maximum at the Pd loading of 4.0%. In contrast, the molar percentages of both Pd(IV) and Pd(II) kept increasing with the increased Pd loading. If revisiting the catalytic efficiencies of PdO/CeO_2 calcined at different temperatures (Fig. 3A), it appears that the catalyst activity was pertinent to the molar percentage of surface Ce(III) (Table 2). However, the catalytic activity of CeO_2 alone was much lower (Fig. 4) although its surface Ce(III) molar percentage and BET surface area were relatively high (Tables 1 and 2). Therefore, Ce(III) alone could not account for the fast degradation of PA in the catalytic ozonation with PdO/CeO_2.

It was reported that Pd(II) could effectively complex with organic compounds [17,18], e.g., carboxylate. Similarly, Pd(II) may also combine with PA and thus affect its catalytic degradation. Therefore, the catalyst activity may be closely related to the surface contents of both Ce(III) and Pd(II). The molar ratio of surface Ce(III)/Pd(II) in all the prepared PdO/CeO_2 catalysts ranged from 0.4 to 3.4 (Table 2). It was noticed that a molar ratio of surface Ce(III)/Pd(II) around 1 (e.g., 0.7–1.3) exhibited a high catalytic activity, while either higher (2.0 or 3.2) or lower (0.4) molar ratios corresponded to a decreased activity of the catalyst. Considering the optimal ratio of surface Ce(III)/Pd(II) as well as the synergetic effect of cerium and palladium oxides that was manifested in the catalytic oxidation and adsorption of PA, both Ce(III) and Pd(II) appeared to be active sites for the catalytic ozonation. In general, Ce(III) is considered as active sites for producing $^{\bullet}O$ species [19]. Therefore, it is hypothesized that Ce(III) catalyzed ozone decomposition to produce active surface $^{\bullet}O$, while Pd (II) provided active sites for PA adsorption. The two resulting active species could quickly react with each other, leading to the fast degradation of aqueous PA.

According to XPS data analysis, the molar ratios of surface Pd(IV)/Pd(II) in PdO and PdO/CeO_2-4.0%-400 °C were 0.25 (calculated from data in Table S1, Supplementary Information) and 0.52 (Table 2), respectively; and those of Ce(IV)/Ce(III) in CeO_2, CeO_2-2 and PdO/CeO_2-4.0%-400 °C were 1.92 (Table 2), 4.26 (Table S2, Supplementary Information) and 2.57 (Table 2), respectively. The CeO_2-2 was prepared by re-calcining CeO_2 at 400 °C for 3 h, which simulates the CeO_2 in PdO/CeO_2-4.0%-400 °C that was calcined twice during synthesis. The surface molar ratio of Ce(IV)/Ce(III) had an increase of 2.34 in the bare CeO_2 after re-calcination, in comparison to an increase of 0.65 in PdO/CeO_2-4.0%-400 °C after Pd was loaded onto CeO_2. Meanwhile, the surface molar ratio of Pd(IV)/Pd(II) increased from 0.25 in PdO to 0.52 in PdO/CeO_2-4.0%-400 °C. Therefore, the Pd loading process increased the surface Pd valence but decreased the surface Ce valence in PdO/CeO_2, indicating that electrons may have transferred from Pd(II) to Ce(IV) during the preparation of the catalyst. This agrees with the standard redox potentials of Pd(IV)/Pd(II) (0.60 V [20]) and Ce(IV)/Ce(III) (1.61 V [21]). Therefore, the electron transfer between CeO_2 and PdO may also contribute to their synergetic effect in catalytic ozonation.

Table 3
Zeta potentials and pH_{pzc} of the prepared catalysts.

Catalysts	Zeta potential (mV)[a]	pH_{pzc}
CeO_2	17.0 ± 0.3	6.3
PdO/CeO_2-4.0%-400 °C	23.2 ± 4.1	5.4
PdO/CeO_2-4.0%-550 °C	26.6 ± 1.0	5.4
PdO/CeO_2-4.0%-650 °C	17.4 ± 0.6	5.0
PdO/CeO_2-4.0%-800 °C	19.5 ± 3.5	5.3
PdO/CeO_2-0.6%-400 °C	16.3 ± 0.4	5.6
PdO/CeO_2-1.8%-400 °C	21.8 ± 3.0	5.4
PdO/CeO_2-4.7%-400 °C	11.4 ± 3.6	5.0

[a] Zeta potential was measured at the same catalyst dose and pH as used in catalytic ozonation.

4.2. Surface charging state and catalytic activity

Compared to CeO_2, the Pd loading process decreased the pH_{pzc} of the prepared catalysts (Table 3). It is known that pH_{pzc} directly reflects the acidic dissociation of surface hydroxyl groups formed on metal oxides in water [22]. Since Pd(II) was a soft Lewis acid while Ce(IV), Ce(III) and Pd(IV) are hard Lewis acids, Pd(II) has a weaker affinity for water and OH^- (hard Lewis bases) to form surface hydroxyl groups [23]. As discussed above (Section 4.1), the electrons could transfer from Pd(II) to Ce(IV) to produce more Ce(III) and Pd(IV) during the Pd loading process, thus changing the acidity of the metal-combined hydroxyl groups. This seems to be responsible for the decrease in the pH_{pzc} of the prepared PdO/CeO_2 catalysts.

By measuring the zeta potentials of catalysts (Table 3), it was found that the PdO/CeO_2 catalysts were positively charged under the applied experimental conditions (pH 4.7). The PdO/CeO_2 calcined at 400 and 550 °C had a relatively higher zeta potential and also exhibited a higher catalytic activity (Fig. 3A). As the Pd loading content of different catalysts was concerned, the zeta potential (Table 3) was also positively correlated with the catalytic activity (Fig. 4A). Therefore, a positively charged surface of PdO/CeO_2 was important for the effective degradation of PA in catalytic ozonation. With its pK_a being 2.49 [24], PA existed predominantly in the deprotonated form (denoted ad PA^-) in water at pH 4.7, so the electrostatic attraction may primarily account for the adsorption of PA onto the catalyst surface.

The zeta potentials of PdO/CeO_2-4.0%-400 °C at pH values of 3.0, 4.7, 6.0, 7.4 and 8.8 were measured to be 18.5, 23.2, −8.9, −15.5 and −29.8 mV, respectively. The increase in OH^- concentration enhanced the electrostatic attraction of OH^- by the catalyst surface, thus decreasing the zeta potential as well as the surface affinity of PdO/CeO_2 for PA^-. On the contrary, a low pH would favor the electrostatic attraction between PdO/CeO_2 and PA^-. The change in the surface charging state of PdO/CeO_2 seemed to account for the difference in its catalytic activity under different pH conditions.

5. Conclusions

In comparison to ozonation alone, the catalytic ozonation with PdO/CeO_2 substantially improved PA degradation in water. To achieve fast degradation of PA, the optimal calcination temperature for PdO/CeO_2 was 550 °C, and the optimal Pd loading was 4.0%. If considering the tradeoff between catalytic activity and energy consumption, the calcination temperature of 400 °C was probably more feasible. The deposited PdO and the support CeO_2 functioned synergistically in the catalytic ozonation. The activity of PdO/CeO_2 was closely related to the molar ratio of surface Ce(III)/Pd(II) and the surface charging state. As the surface molar ratio of Ce(III)/Pd(II) approached 1, PdO/CeO_2 exhibited a high catalytic activity. The positive surface charging state of PdO/CeO_2, which could be attained at acidic pHs (e.g., 4.7), was necessary for the efficient degradation of PA in catalytic ozonation.

PdO/CeO_2 was proved to be a highly effective catalyst to enhance the ozonation of PA in water. However, more studies are still needed to clarify the catalytic mechanisms regarding the subtle interactions among the surface metals, ozone and PA. In addition, PdO/CeO_2 may have a prospective application in catalytic degradation of other organic compounds (e.g., natural organic matter in source water) by ozone, which also needs further study.

Acknowledgements

The authors greatly appreciate the financial supports from the National Natural Science Foundation of China (Project # 20837001, 50921064, and 50708108) and the Ministry of Science and Technology of China (Project # 2008AA06A414 and 2008ZX07421-004).

Appendix A. Supplementary data

Supplementary data associated with this article can be found, in the online version, at doi:10.1016/j.molcata.2011.08.003.

References

[1] V. Camel, A. Bermond, Water Res. 32 (1998) 3208–3222.
[2] Z.M. Qiang, C. Adams, R. Surampalli, Ozone Sci. Eng. 26 (2004) 525–537.
[3] B. Kasprzyk-Hordern, M. Ziolek, J. Nawrocki, Appl. Catal. B Environ. 46 (2003) 639–669.
[4] Z.M. Qiang, C. Liu, B.Z. Dong, Y.L. Zhang, Chemosphere 78 (2010) 517–526.
[5] F.J. Beltran, B. Acedo, F.J. Rivas, O. Gimeno, Ozone Sci. Eng. 27 (2005) 159–169.
[6] P.M. Alvarez, F.J. Beltrán, J.P. Pocostales, F.J. Masa, Appl. Catal. B: Environ. 72 (2007) 322–330.
[7] R. Andeozzi, V. Caprio, A. Insola, R. Marotta, V. Tufano, Water Res. 32 (1998) 1492–1496.
[8] N.K.V. Leitner, H. Fu, Top. Catal. 33 (2005) 249–256.
[9] F.J. Rivas, M. Carbajo, F.J. Beltrán, B. Acedo, O. Gimeno, Appl. Catal. B: Environ. 62 (2006) 93–103.
[10] L.L. Xu, Z.M. Li, Q.H. Cai, H.X. Wang, H. Gao, W. Lv, J. Liu, CrystEngComm 12 (2010) 2166–2172.
[11] H.S. Kim, H. Lee, K.S. Han, J.H. Kim, M.S. Song, M.S. Park, J.Y. Lee, J.K. Kang, J. Phys. Chem. B 109 (2005) 8983–8986.
[12] J. Hoigne, H. Bader, Water Res. 15 (1981) 449–456.
[13] B. Wen, J.F. Jia, W.M.H. Sachtler, J. Phys. Chem. B 106 (2002) 7520–7523.
[14] C.J. Liu, K.L. Yu, Y.P. Zhang, X.L. Zhu, F. He, B. Eliasson, Appl. Catal. B Environ. 47 (2004) 95–100.
[15] C. Koravik, S. Patil, S. Seal, W.T. Self, Chem. Commun. 10 (2007) 1056–1058.
[16] P.C.C. Faria, J.J.M. Orfao, M.F.R. Pereira, Catal. Commun. 9 (2008) 2121–2126.
[17] A. Garoufis, S.K. Hadjikakou, N. Hadjiliadis, Coord. Chem. Rev. 253 (2009) 1384–1397.
[18] S. Hermans, M. Wenkin, M. Devillers, J. Mol. Catal. A Chem. 136 (1998) 59–68.
[19] A. Naydenov, R. Stoyanova, D. Mehandjiev, J. Mol. Catal. A Chem. 98 (1995) 9–14.
[20] L.H.D. Antonia, G. Tremiliosi-Fiho, G. Jerkiewicz, J. Electroanal. Chem. 502 (2001) 72–81.
[21] B. Fang, S. Iwasa, Y. Wei, T. Arai, M. Kumagai, Electrochim. Acta 47 (2002) 3971–3976.
[22] W. Stumm, Chemistry of the Solid–Water Interface: Processes at the Mineral-Water and Particle-Water Interface in Natural Systems, Wiley-Interscience, New York, 1992, pp. 13–21.
[23] P.W. Ayers, J. Chem. Phys. 122 (2005) 141102–141105.
[24] D. Volgger, A.J. Zemann, G.K. Bonn, M.J. Antal, J. Chromatogr. A 758 (1997) 263–276.